Thermal Analysis Algorithm for Oil and Gas Wells

João Victor Carvalho de Mattos^{1*}, Márcio de Melo Araújo¹, José Fábio Abreu de Andrade¹

**ISENAI CIMATEC University; Salvador, Bahia, Brazil

Thermal failures are common in oil and gas well structures, since they operate under extreme temperatures. Therefore, it is essential to investigate the thermal factors that can lead to failures in order to prevent accidents. This article presents an innovative thermal analysis method, based on steady-state heat exchanges, simulated using a Microsoft Excel algorithm to calculate the heat exchange processes among well components. The results proved to be adequate, illustrating numerically and graphically two operation scenarios proposed for the well. Therefore, it serves as an alternative to meet the growing demand for studies on thermal failures in the oil and gas industry.

Keywords: Oil and Gas. Wells. Structure Failures. Heat Exchange.

Oil and gas wells typically operate at high temperatures, either due to the heated fluids used or the geothermal properties of the geological formation in which the well is located [1,2]. These circumstances directly affect the components of a sound system, leading to mechanical and structural failures [3]. Those failures are, in part, due to thermal factors, as temperature or thermal gradients at the well's components generate stresses and deformations, increasing the likelihood of accidents [4-6]. Well casings are commonly affected by these thermal factors, being critical for oil and gas production; therefore, an operational well must have a casing project with a thorough thermal analysis [7].

Therefore, it is helpful to develop studies and methods that focus on analyzing the factors involved in these thermal failure processes, thereby minimizing the effects and accidents related to thermal reactions in oil and gas well operations [8-10]. This study presents a method, developed as a Microsoft Excel algorithm, for analyzing the effects of temperature on the components of an onshore laboratory well project, designed for testing in the oil and gas industry. This algorithm

Received on 18 May 2025; revised 21 July 2025. Address for correspondence: João Victor Carvalho de Mattos. Av. Orlando Gomes, 1845 - Piatã, Salvador – BA – Brazil, Zip Code: 41650-010. E-mail: joao.mattos@aln.senaicimatec. edu.br.

J Bioeng. Tech. Health 2025;8(4):370-375 © 2025 by SENAI CIMATEC University. All rights reserved.

aims to simulate the heat exchanges in a test well, facilitating thermal analysis of the structure and verifying the factors involved in the process. It calculates the temperature of the components applied to optimize a well project. In this case, the method was primarily applied to the analysis of well casing design.

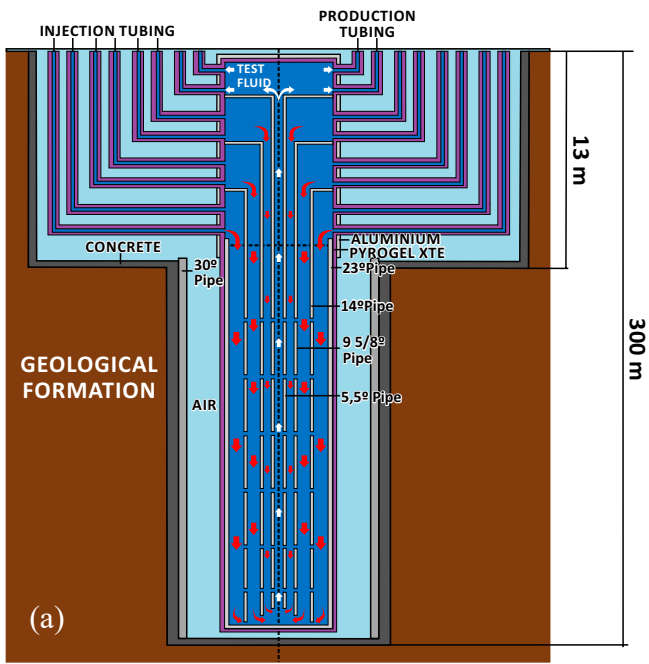
Materials and Methods

Well Description

In this work, the project of a 300 m well with a 13 m wellhead subsurface chamber was analyzed. Figure 1a presents a simplified model of the system considered for the calculations, consisting of: casing and pipes (in gray), two layers of insulation (in light gray and purple), a layer of cementation concrete (In black), the geological formation (In brown), the layers of air between in the well (In light blue) and a water-based test fluid (In dark blue).

Figure 1b illustrates the layout used for the cells in Microsoft Excel software, and their position, as an example for calculating the equilibrium temperature in the well. Each line represents 0.1 m of the well length, and each column one of its components. In this figure, the orange cells represent the masses whose equilibrium temperatures are being calculated. In contrast, the blue cells illustrate the masses whose temperatures influence the calculation of the equilibrium temperature at the determined orange cell.

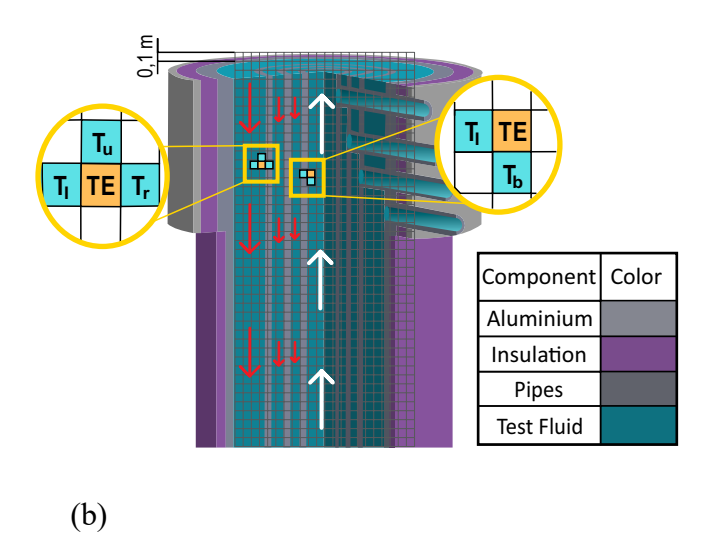
Figure 1. 2D layout of main well components and cell arrangements for calculations.



Thus, this well is a system composed of injection pipes connected laterally to different fluid spools, which are arranged above a 23-inch-diameter and 2-inch-thick steel tube that extends to the bottom of the well. Figure 1a shows fluid flow directions at healthy injection (red arrows) and production (white arrows) operations. The fluid is injected laterally, and the production consists of the passage of the fluid to the central tube and its return to the surface. To simplify the calculations without compromising the accuracy of the results, it was assumed that the fluid operates in a permanent flow regime and that the process experiences no thermal variation due to the mixing of fluids at different temperatures, only through heat exchanges. In this analysis, two scenarios were considered for the injection of heated and cooled test fluid, with different initial temperatures for each case: 150 °C for the first scenario and 4 °C for the second.

Calculation Model

The basis of the model calculation is the fluid's thermal energy, which is transferred or received, depending on the fluid temperature, to all other components through heat exchange processes.



These are categorized as conduction for both the processes between the formation, concrete, and 30" pipe, as well as for the insulation and the 23" pipe. Additionally, they are categorized as convection for those that occur between the air and the insulation, as well as for the fluid and the pipes. It was assumed that the heat flow in the well follows the same direction as the fluid flow, while spreading horizontally throughout the system.

To adapt these concepts to the calculations and the algorithm created in Microsoft Excel, the well length was segmented into a grid of cells, as shown. The temperature of each cell was calculated using the equations (1) and (2), according to its respective scenario, where T1 is the component initial temperature, "c" its specific heat, "m" its mass and the subscripts "u", "r", "l" and "b" to refer the terms respectively to the cells in the upper, right, left and bottom layer of the one whose equilibrium temperature (TE) is calculated [11].

$$T_E = \frac{m_u \cdot c_u \cdot T_u + m_r \cdot c_r \cdot T_r + m_l \cdot c_l \cdot T_l}{m_u \cdot c_u + m_r \cdot c_r + m_l \cdot c_l} (Injection) (1)$$

$$T_E = \frac{m_b \cdot c_b \cdot T_b + m_l \cdot c_l \cdot T_l}{m_b \cdot c_b + m_l \cdot c_l} (Production)$$
 (2)

Boundary Conditions

Considering the system as isolated, the maximum and minimum input temperatures were used as boundary conditions for the analysis, which was then used to calculate the temperature for the components that undergo heat exchange processes with others during operation.

The temperature of the geological formation at the end of the system was calculated as a function of the geothermal gradient, which is the rate of variation of soil temperature with depth (h), as shown in Eq. 3. In this study, an ambient temperature was considered a temperature of 25 °C [12] and a geothermal gradient (GT) of 0.025 °C/m [13].

$$TF = 25^{\circ}C + GT \cdot h \tag{3}$$

The air temperature inside the well also does not present significant changes, as this layer of air is not trapped inside the structure. Therefore, it continuously undergoes a convection process with the external air, continually renewing itself and dissipating the accumulated heat, maintaining an ambient temperature of 25 °C.

Calculation Algorithm

The algorithm follows the logic presented in Figure 2 to reproduce the cited calculations.

To obtain accurate results using Excel, the "Iterative Calculation" and "Circular Reference" functions were applied. From this data, graphs were

created that illustrate the temperature distribution of the well components according to depth, representing the actual geometric arrangement of the elements present in the system. This was achieved by inserting the calculated temperature data into the cells of a separate spreadsheet, organized to illustrate the well's component arrangement, and applying the Microsoft Excel "Conditional Formatting" function to them, which correlates cell values to a color pattern defined by the user.

Results Validation

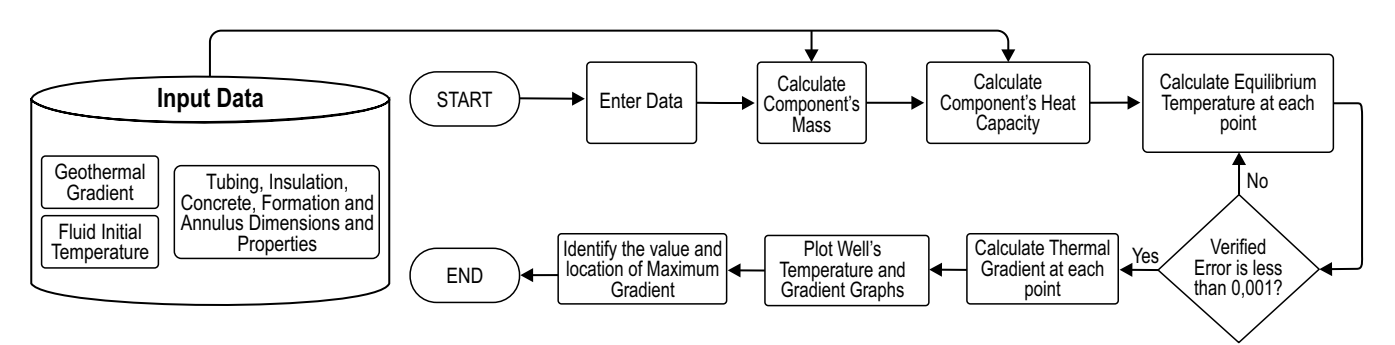
To minimize possible numerical errors or due to assumptions considered in relation to the algorithm, the temperatures of the 23" tube surfaces were analytically calculated. We calculated the total heat capacity of the system based on the thermal resistances of each component. Equation 6 was used to calculate the total heat capacity, with T_{max} and T_{amb} representing the maximum and minimum temperatures present, respectively. Equation 7 was used to define the temperature of the external surface of the tube [14]. Comparing the results of the equations with the temperature values obtained through the algorithm, it was possible to verify the accuracy of the developed method.

$$Q_{t=\frac{T_{max}-T_{amb}}{R_t}} \tag{3}$$

$$T_{ext} = T_{max} - Q_t \cdot R_{tube} \tag{4}$$

To verify the accuracy of the elaborated algorithm once more, a mesh convergence study

Figure 2. Flowchart of the developed calculation algorithm.



was conducted, in which other discretization parameters were applied in relation to the software grid line, with the lines representing 0.2 m and 0.5 m of the well length, unlike the 0.1 m used as the standard originally. After all, the results of each model were verified and compared.

Results and Discussion

In Scenario 1, as depicted in Figure 3, a liquid solution is injected at 150 °C into the well. At the operation's initial instant (Figure 3a), it is already possible to identify, in yellow, a slight heating in the produced fluid, due to its contact with the annular sections already filled with test fluid. Similarly, at the medium and final instant (Figure 3b and 3c,

respectively), the produced fluid tends to heat until it reaches a temperature closer to that of the injected fluid. Thus, there is a tendency for the temperature of the well elements to increase after the passage of the fluid, as continuous injection causes the system components to heat up. The thermal gradients acting in the casing were calculated by subtracting the external surface temperature from the internal surface temperature at each point along the pipe.

In Scenario 2, shown in Figure 4, a fluid is injected at 4 °C, exhibiting a behavior similar to that observed in Scenario 1, with the thermal gradient calculated in the same manner. However, in this case, the fluid inlet temperature is lower than the ambient temperature, and the other components tend to cool through their passage, reaching a final temperature of 4 °C.

Figure 3. Well temperature profile in Scenario 1.

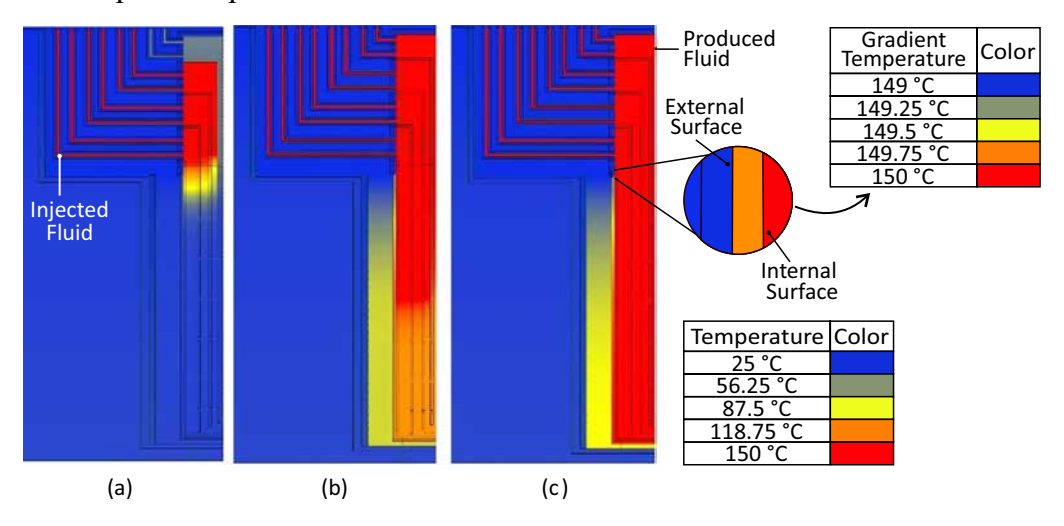
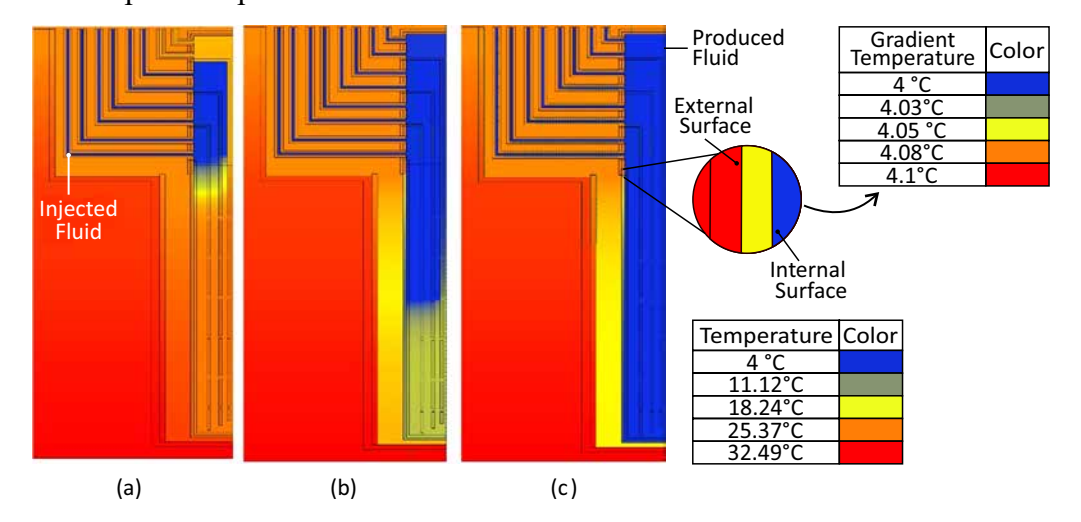


Figure 4. Well temperature profile in Scenario 2



Thus, it was possible to verify the temperature of each point of the structure, as well as the thermal gradient acting on them. The behavior of the thermal gradients acting on the casing was calculated for the final instants of both scenarios and shown in Figure 5, according to their respective inlet temperatures. Those instants are considered critical because all the annular spaces are filled with and at the temperature of the injected fluid, which brings the internal temperature of the casing near the boundary conditions for each situation.

The maximum gradients were identified at the top of the casing, primarily because this region is in contact simultaneously with the air at ambient temperature and with the injected fluid on its external and internal surfaces, respectively. This increases the temperature difference between those surfaces and maximizes the gradient. Scenario 1

presents a greater gradient because the fluid injected at 150 °C differs more from the air at 25 °C than the fluid at 4 °C, as in Scenario 2. This indicates that the maximum stresses are acting on this location, since thermal stress is directly proportional to the temperature gradient, classifying it as the critical region of the structure [15].

The validation test consisted of comparing the percentage divergence between the casing external surface temperature at the critical region calculated analytically using the mesh divergence models and by the algorithm, both of which were informed by Table 1.

Thus, the maximum difference calculated, considering both operation scenarios, did not exceed 1,88%, which is considered a divergence that did not significantly affect the results obtained, certifying the accuracy and viability of the developed method.

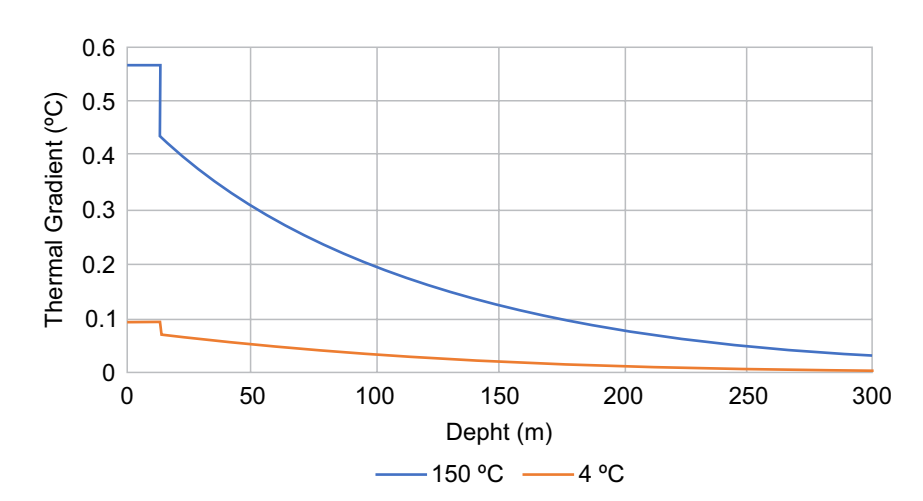


Figure 5. Thermal gradients acting on the well's casing at operation.

Table 1. Percentage divergence for each analyzed test model.

Test Model	Calculated Temperature		Standard Model Temperature		Percentage Divergence	
	Scenario 1	Scenario 2	Scenario 1	Scenario 2	Scenario 1	Scenario 2
Analytical	149.4421 °C	4.0937 °C	149.4269 °C	4.0962 °C	0.01%	0.06%
0.2 m Mesh	149.7128 ℃	4.0482 °C			0.19%	1.17%
0.5 m Mesh	149.8850 °C	4.0193 °C			0.31%	1.88%

Conclusion

This study verified the behavior and influence of thermal factors on the structure of a laboratory well, identifying that the test fluid and the geological formation are the components that govern heat exchanges during operation. This means that the elements adjacent to them tend to reach thermal equilibrium at a temperature similar to their own.

A layer of non-trapped air is identified inside the well, acting as a heat sink that constantly transports air from the bottom of the well to the surface. Using the algorithm presented, it was possible to illustrate the thermal behavior of the well's components and accurately calculate the temperatures of each component in the system, as well as the thermal gradient in the well's casing. This allowed verification of the critical region and facilitated the analysis of the system's safety during operation. Thus, this proves that the developed method is a suitable technique for thermal analyses of wells, serving as an alternative to optimize analyses for projects and utilize robust software, providing a simple and innovative solution to mitigate failures and accidents. More studies have been conducted on the method presented in this article, including an analysis of the stresses acting on the well components, particularly on the casing, to determine possible failure modes for the structure and assess whether the project meets the required standards. It is intended to complement this work in the future, making it an applicable method for well projects in the oil and gas industry.

Acknowledgments

We thank to the Brazilian National Agency of Petroleum, Natural Gas and Biofuels (ANP), the ANP Human Resources Program (PRH 27.1), and to the SENAI CIMATEC.

References

- 1. Zhi Z, Wang H. Effect of thermal expansion annulus pressure on cement sheath mechanical integrity in HPHT gas wells. Appl Therm Eng. 2017;118:600–11.
- 2. Thorbjörnsson I, Kaldal GS, Ragnarsson Á. Testing flexible couplings for geothermal wells. Palm Springs: GRC; 2019.
- Thorbjornsson I, Kaldal GS, Gunnarsson BS, Ragnarsson Á. A new approach to mitigate casing failures in hightemperature geothermal wells. ISOR, Iceland. GRC Trans. 2017;41.
- 4. Maharaj G. Thermal well casing failure analysis. In: SPE Latin America/Caribbean Petroleum Engineering Conference; Apr 1996; Port-of-Spain, Trinidad.
- 5. Zhi Z, Wang H. Effect of thermal expansion annulus pressure on cement sheath mechanical integrity in HPHT gas wells. Appl Therm Eng. 2017;118:600–11.
- 6. Chen L, Yu W, Lu Y, Wu P, Han F. Characteristics of heat fluxes of an oil pipeline armed with thermosyphons in permafrost regions. Appl Therm Eng. 2021;190:116694.
- 7. Chilingarian GV, Rahman SS. Casing design theory and practice. Amsterdam: Elsevier; 1995.
- 8. Zhang B, Guan Z, Hasan AR, Lu N, Wang Q, Xu Y, et al. Development and design of new casing to mitigate trapped annular pressure caused by thermal expansion in oil and gas wells. Appl Therm Eng. 2017;118:292–8.
- Cao X, Deng Z, Nian Y. Evaluation of annual performances of crude oil pipeline transportation by solar heating. Appl Therm Eng. 2024;245.
- Fei Z, Li Y, Liu Z, Tang Y. Flow and heat transfer characteristics of oil-based drilling cuttings in a screwdriving spiral heat exchanger. Appl Therm Eng. 2020;181.
- 11. Incropera FP, DeWitt DP. Fundamentos de transferência de calor e de massa. 5th ed. Rio de Janeiro: LTC; 2003.
- 12. Lillo M, Suárez F, Hausner MB, Yáñez G, Veloso EA. Extension of duplexed single-ended distributed temperature sensing calibration algorithms and their application in geothermal systems. Sensors. 2022;22(9):3319.
- 13. Toledo MCM. Estrutura interna da Terra. São Paulo: USP/UNIVESP/EDUSP; 2014.
- 14. Çengel YA, Ghajar AJ. Transferência de calor e massa: uma abordagem prática. 4th ed. 2012.
- 15. Young WC, Budynas RG. Roark's formulas for stress and strain. 7th ed. New York: McGraw Hill; 2001.